Mars Observer Orbit Determination Analysis

Pasquale Esposito* and Duane Roth†
Jet Propulsion Laboratory, California Institute of Technology, Pasadena, California 91109
and
Stuart Demcak‡
OAO Corporation, Altadena, California 91001

Orbital accuracies throughout the Mars Observer mission are summarized and a plan is developed for achieving navigation objectives. These objectives are 1) to navigate the Mars Observer spacecraft to Mars and achieve accurate targeting at Mars, 2) to propulsively maneuver the spacecraft into a three-day period, capture orbit, 3) to navigate the spacecraft into a short-period (1.96 h), low-altitude, nearly circular mapping orbit, and 4) to maintain Mars Observer in the mapping orbit throughout 687 days devoted to scientific data acquisition. During the orbital phase, gravity field and atmospheric drag perturbations will control the spacecraft's orbital evolution. They are also the major factors influencing the accuracy of the prediction and reconstruction of the spacecraft's orbital motion. Initially, the current best estimate of the Mars gravitational field model will be used during flight operations. However, this will be superseded by a 20th degree and order model developed by the navigation team early in the mapping phase. With this implementation, spacecraft reconstructed position errors will be improved significantly. In addition, estimates of the average atmospheric density (over four to five orbits) will be possible throughout Mars' perihelion.

Nomenclature

a = orbital semimajor axis
e = orbital eccentricity
GM = gravitational constant (Newtonian gravitational constant times the mass of a planet)
I = orbital inclination
P = orbital period
r = position of the spacecraft
r_s = tracking station distance perpendicular to the Earth's rotational axis
R = radial component of position
S = sensitivity matrix
v = velocity of the spacecraft
W = tracking data weight matrix
Z = tracking station distance perpendicular to the Earth's equatorial plane
Λ = estimated parameter covariance matrix
$\tilde{\Lambda}$ = a priori estimated parameter covariance matrix
Λ_c = consider parameter covariance matrix
$\tilde{\Lambda}_c$ = a priori consider parameter covariance matrix
λ = tracking station longitude
Ω = longitude of the ascending mode
ω = argument of periapsis

Introduction

THIS paper provides a summary of the results of a simulated orbit determination analysis throughout the Mars Observer mission. For this work, the mission has been divided into three phases: interplanetary cruise, orbit insertion, and mapping. This has been done because of the different objectives to be achieved during each phase and because the dominant orbital error sources vary from phase to phase. The duration and dates associated with each phase are given in Table 1.

Received Dec. 20, 1989; revision received July 12, 1991; accepted for publication July 12, 1991.

*Technical Manager, Navigation Systems Section.
†Member of Technical Staff, Navigation Systems Section.
‡Orbit Determination Engineer, 787 W. Woodbury Rd.

During the interplanetary cruise, the major objective is to target the spacecraft to a nominal Mars aim point that is over the north polar region at an encounter altitude of approximately 565 km. This will ensure capture into a three-day period, elliptic orbit as a result of the Mars orbit insertion propulsive maneuver. During the orbit insertion phase, a sequence of maneuvers takes the spacecraft from the initial, highly elliptic capture orbit to the near-circular mapping orbit. Finally, during mapping, orbit determination analysis is required to assess reconstructed and predicted spacecraft position and velocity errors.

Targeted orbit elements for both the initial capture orbit and the mapping orbit are given in Table 2.

Note that the mapping orbit is short periodic, nearly circular, and Sun synchronous. Previous U.S. orbiters were long periodic and very eccentric, as indicated in Table 3.

Navigation Tracking Data

Two-way coherent Doppler and round-trip, time-delay measurements are the primary data used for navigating the Mars Observer spacecraft. The former measures the radial component of velocity between the Earth-based tracking station and the spacecraft and is usually called range rate. The latter measures the station-to-spacecraft distance and is called range.

These measurements are usually made continuously at a Deep Space Network (DSN) tracking station for the duration of a tracking pass (that is, from spacecraft rise until the spacecraft sets, which typically amounts to 8–10 h). During interplanetary cruise, intense periods of navigation data acquisition occur during the first 30 days after launch and again for the last 30 days before the Mars encounter. During these two intervals, data will be acquired continuously. Thus, three DSN stations per day are required to receive this data. One station from each of the three Deep Space Station (DSS) complexes, which are separated by about 120° in longitude, will participate. These are DSS-15 at Goldstone, California, DSS-45 near Canberra, Australia, and DSS-65 near Madrid, Spain. Continuous measurements during the first 30 days are required to evaluate the results of the injection propulsive maneuver, to determine the postinjection orbit of the spacecraft, and to prepare for the execution of the first trajectory correction maneuver. The injection maneuver causes the spacecraft to depart from its Earth orbit and to be placed into a solar orbit that

Table 1 Mars Observer mission time line

Event	Earliest launch	Latest launch
Launch period, 20 days	Sept. 16, 1992	Oct. 5, 1992
Mars orbit insertion (MOI)	Aug. 19, 1993	Sept. 5, 1993
Orbit insertion phase duration, days	118	97
Start mapping data acquisition	Dec. 16, 1993	Dec. 11, 1993
End of mapping	Nov. 3, 1995	Oct. 29, 1995

Table 2 Mars Observer orbit elements

Orbit element	Capture orbit	Mapping orbit
Semimajor axis a, km	42,000	3775.334
Eccentricity e	0.906	0.0072
Inclination I, deg	92.865	92.865
Argument of periapsis ω, deg	119.355	−90.0
Longitude of ascending node Ω, deg	29.178	34.866
Orbital period P, h	72.6	1.96
Epoch	Aug. 19, 1993	Nov. 29, 1993

Table 3 Mariner and Viking orbit elements

Orbit element	Mariner 9	Vikings 1 and 2
Eccentricity	0.62	0.75
Period, h	12	24

Table 4 Navigation data accuracy requirements

Tracking data	Accuracy, 1 σ
Two-way coherent Doppler (60-s average), mm/s	0.20
Round-trip travel time or range, m	5.0
ΔVLBI angular measurement, nrad	50.0

shall encounter Mars after 337 days of interplanetary cruise. Continuous data during the last 30 days of cruise are required to prepare for the final targeting maneuver [trajectory correction maneuver (TCM-4)] at encounter minus 15 days, to evaluate the results by orbit determination, and to prepare for the Mars capture maneuver called Mars orbit insertion (MOI). Between these two intense periods of tracking, navigation data are generally acquired at one tracking pass per day.

For Mars Observer, Doppler and range data shall be acquired at an X-band frequency (transmitted frequency $\sim 7.2 \times 10^9$ Hz). However, for many previous missions, telecommunications used an S-band frequency ($\sim 2.1 \times 10^9$ Hz). This increase in frequency reduces the influence of the Earth's ionosphere and interplanetary plasma in the radio tracking data.

A third type of data called very long baseline interferometry (VLBI) and differenced VLBI shall also be used during the interplanetary cruise to make precise angular measurements of the location of the spacecraft.[1,2] As before, this is an Earth-based measurement by which signals transmitted from the spacecraft are received simultaneously at two DSN stations. The difference in the arrival times of the signals is determined, which, along with an accurate knowledge of the baseline, allows one to calculate the angular direction to the spacecraft. The accuracy associated with each of these data is given in Table 4.

Orbit Determination for Mars Targeting

During the 337-day interval between launch and Mars encounter, simulated orbit determination analyses using the data previously described have been conducted. The interplanetary cruise, starting with the first launch date, has been subdivided into five sections. These are separated by the occurrence of four propulsive maneuvers identified as trajectory correction maneuvers (TCM). The error sources influencing interplanetary navigation are summarized as follows.

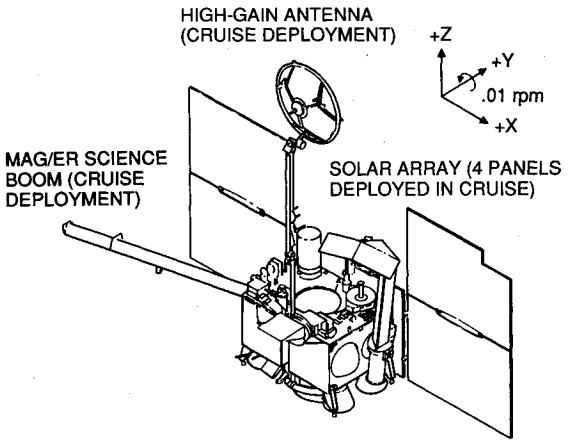

Fig. 1 Mars Observer spacecraft configuration during interplanetary cruise.

The location and errors associated with the DSN stations previously mentioned must be known. These are specified in cylindrical coordinates and are referred to as longitude, distance from the Earth's rotational axis, and height with respect to the Earth's equatorial plane. Knowledge of the position and velocity of the target (Mars) and the Earth from which the data measurements are referenced is also required. This is referred to as the Earth-Mars planetary ephemeris. The corresponding errors can be given in position and velocity or orbit elements for both planets. In addition to the standard deviations, the correlations between the orbit elements are also required, giving rise to the need for a 12 × 12 covariance matrix for the complete specification of errors.

During cruise, the solar radiation pressure exerts a major perturbation influencing the spacecraft's motion. The spacecraft's cruise configuration is shown in Fig. 1. Individual solar panels measure 72 in. × 88.25 in. (1.83 m × 2.24 m) and the high-gain antenna (HGA) has a diameter of 1.5 m. After injection, the mass of the spacecraft is approximately 2487 kg. The major component of the solar radiation pressure (SRP) acceleration is in the radial direction (Sun to spacecraft) with much smaller effects perpendicular to this direction.

Spacecraft self-induced accelerations refer primarily to the process whereby accumulated angular momentum (stored in reaction wheels) is desaturated. To maintain the spacecraft's attitude, small thrusters will be fired during desaturation, resulting in a net acceleration experienced by the spacecraft. On average, desaturations will occur once per week during cruise, and a single desaturation event will occur in a pulsed-mode requiring several minutes. For previous spacecraft, gas leakage has also been a source of a self-induced force. Should this occur on Mars Observer, the navigation team is prepared to model this perturbative acceleration as either a constant, linear, or exponential acceleration.

During the near Earth departure and Mars approach, the Newtonian force will dominate the spacecraft's motion. Thus the values of the planetary gravitational constants and their inherent errors are important in any simulations in which Mars targeting accuracies are being evaluated.

Lastly, the angular coordinates of radio sources used to acquire VLBI data are required. The errors in these coordinates are just as important to estimate this effect on spacecraft location and targeting at Mars.

The 1-σ a priori error for all these effects that influence the accuracy with which we can monitor and determine the space-

craft's motion are summarized in Table 5. The errors in the gravitational constants are somewhat conservative. Recent analyses indicate that 1-σ uncertainties are 0.001 km^3/s^2 and about 0.08 km^3/s^2 for the gravitational constants of Earth and Mars, respectively.[3,4]

During interplanetary cruise, one of our major objectives is to target the spacecraft to a predetermined Mars encounter aim point. The errors associated with this targeting are just as important. This information is needed years before launch to refine the mission design process and to guide the navigation team during actual flight operations. The methodology of this simulation of interplanetary cruise operations is 1) to acquire simulated Doppler, range, and VLBI data according to the tracking schedule expected to be in place during flight operations, 2) to generate a nominal Earth-to-Mars interplanetary trajectory in which the spacecraft encounters Mars at the nominal aim point (this process involves a numerical integration of the spacecraft's equations of motion in which all known forces are either acting on the spacecraft or are simulated in the analysis), 3) to analyze this simulated data using orbit determination software that employs a least-squares algorithm to fit the data and to correct model parameters (e.g., initial conditions, SRP constants, etc.) as necessary, and 4) to determine the spacecraft's position and velocity errors along the nominal trajectory. These errors can also be propagated to encounter and transformed into different coordinate systems to aid in the analysis. For example, at encounter we employ a target coordinate system (called the B plane) to monitor the accuracy of the targeting and to correct the spacecraft's motion (via propulsive maneuvers) as required. Orbit determination targeting errors associated with each of the four planned TCMs are given in Table 6. Four sets of B-plane errors are given because the 337-day cruise interval has been divided into five subphases delineated by the occurrence of a TCM. Currently, these subphases have been treated independently. The shape and orientation of each targeted error ellipse are given in Fig. 2 along with a representation of the B plane. The aim point is B = 8771 km from Mars and is located over the northern polar region (ϕ = −92.3 deg).

Table 5 Navigation error models

Source	A priori error, 1 σ
Station locations (cylindrical coordinates, deg, m, m)	λ = 0.106 × 10^{-4} r_s = 0.71 Z = 10.0
Solar radiation pressure (% of the effect)	radial = 10 lateral = 10–20
Spacecraft self-induced accelerations, km/s^2	radial: 3 × 10^{-12} lateral: 3 × 10^{-12} (daily average)
Earth-Mars planetary ephemeris	12 × 12 Covariance matrix radial = 0.25 crosstrack = 49 downtrack = 113 } heliocentric Mars position errors, km
Earth, Moon, and Mars gravitational constants, km^3/s^2	GM (Earth) = 0.05 GM (Moon) = 0.005 GM (Mars) = 0.15
Radio source angular coordinates, rad	167. × 10^{-9}

Table 6 Mars targeting errors due to orbit determination simulation analysis performed throughout interplanetary cruise

Cruise subphase; (duration)	Error ellipse, km, at encounter, 1 σ
Launch, Sept. 16, 1992, through TCM-1; 15 days	2417 × 429
TCM-1, Oct. 1, 1992, through TCM-2; 98 days	578 × 142
TCM-2, Jan. 7, 1993, through TCM-3; 30 days	575 × 151
TCM-3, Feb. 7, 1993, through TCM-4; 179 days	159 × 18
TCM-4 and encounter occur on Aug. 4, 1993, and Aug. 19, 1993, respectively.	

Orbit Determination During the Orbit Insertion Phase

This phase begins at MOI and ends when the spacecraft is declared ready to commence mapping operations (nominally Dec. 16, 1993). Its duration is 118 days, which corresponds to the first launch date. There are four distinct orbits during this phase. Starting with the Mars capture orbit (P = 3 days, e = 0.91), the spacecraft shall be placed into a drift orbit (P = 1 day, e = 0.81) at MOI + 21 days, then into an intermediate orbit (P = 4.2 h, e = 0.40) at MOI + 85 days, and finally into the mapping orbit (P = 1.96 h, e = 0.0072) on Nov. 29, 1993. Near the end of this phase, Doppler data will be acquired to develop a Mars gravity field model suitable for flight operations during the mapping phase. Throughout orbit insertion, Doppler will be acquired continuously.

For design and planning purposes, we have simulated the acquisition of Doppler throughout this phase. The procedure for the analysis of this data is the same as previously described. However, we have added the influence and errors associated with the Mars gravity field and the atmospheric density. Formal errors associated with truncated sixth degree and order field are given in Table 7.[5] These formal errors are optimistic, and so for our simulations we have increased them by a factor of 10 for all terms up to and including the fourth degree and by a factor of 6 for all higher order terms. At-

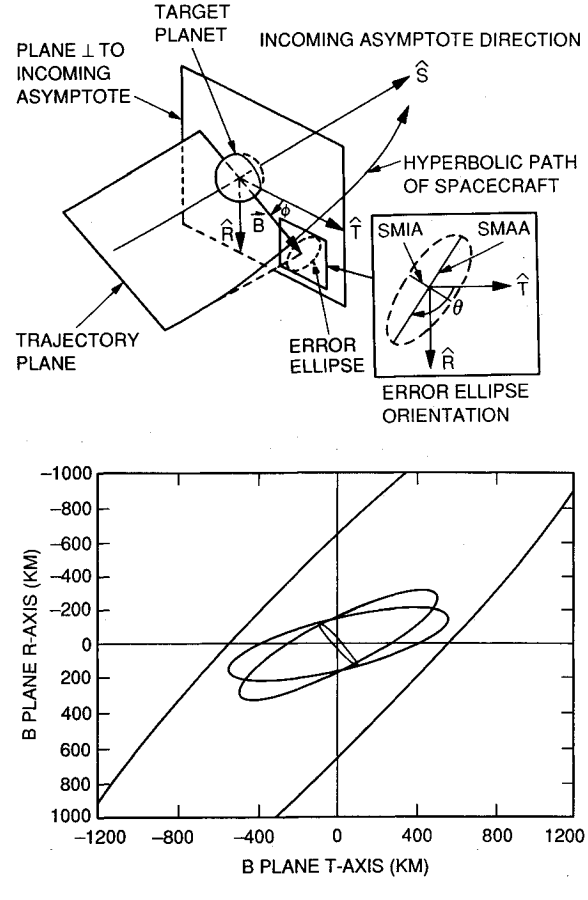

Fig. 2 B-plane description and orbit determination targeting errors for four subphases during interplanetary cruise.

Table 7 Mars gravitational field error model, 1-σ formal error

Unnormalized coefficient		Uncertainty ($\times 10^{-07}$)				
J_2	0.440					
C_{21}, C_{22}	—	0.0572				
S_{21}, S_{22}	—	0.0614				
J_3	1.28					
C_{31},...	0.238	0.0670	0.0183			
S_{31},...	0.231	0.0631	0.0161			
J_4	1.80					
C_{41},...	0.364	0.0746	0.0149	0.00484		
S_{41},...	0.338	0.0743	0.0146	0.00462		
J_5	2.17					
C_{51},...	0.468	0.0674	0.0124	0.00266	0.000709	
S_{51},...	0.491	0.0680	0.0126	0.00275	0.000696	
J_6	2.50					
C_{61},...	0.735	0.0700	0.0120	0.00151	0.00037	0.000079
S_{61},...	0.748	0.0692	0.0121	0.00147	0.00037	0.000075

Table 8 Reconstructed and predicted spacecraft position errors, km, 1 σ, for two cases during the orbit insertion phase

Epoch, T_0; days past T_0	Radial	Cross-track	Down-track	Comment
Aug. 19, 1993	0.016	0.039	0.11	Mars capture orbit (P = 72 h, e = 0.91); Three days of Doppler
11	1.2	0.89	3.0	data were simulated.
Nov. 15, 1993	0.022	1.3	2.0	Intermediate orbit (P = 4.2 h, e = 0.4); Nine hours of Doppler
10	0.39	1.7	8.5	data were simulated.

mospheric drag errors are not significant for orbit determination (OD) until we reach the mapping orbit.

Orbit determination analyses using simulated data, as previously outlined, have been performed throughout this phase. In Table 8 we show the results for two cases. The first involves the Mars capture orbit. Here we simulated continuous Doppler data over three days, which corresponds to one orbit. These data were fit in a least-squares sense, and a set of six initial conditions (i.e., position and velocity or alternatively the six classical orbit elements) at the epoch Aug. 19, 1993, were updated. The errors corresponding to the models previously discussed in Tables 5 and 7 were accounted for. The results of this case expressed in Mars centered position errors (radial, crosstrack, and downtrack) at the epoch of the analysis are shown in Table 8. These errors have not been propagated in time; they are the result of the analysis of Doppler data and are referred to as reconstructed errors. In addition, we show error growth as a result of propagation to 11 days past the epoch (i.e., Aug. 30, 1993). These are referred to as predicted errors. The reason for this propagation is that these OD errors will be used in the design and planning of the first in-orbit maneuver called ECM-1 (elliptic orbit change maneuver).

The results of a second case involving the intermediate orbit are also given. Again we show both reconstructed and predicted errors. For this case, the predicted OD errors are being used to design the TLO-2 (transfer to low orbit) maneuver that occurs on Nov. 22, 1993, in this simulation.

At the end of this phase while the spacecraft is in the mapping orbit, a Mars gravity calibration (GC) plan will be implemented. According to this plan, seven days of Doppler data shall be acquired continuously. During this time, the spacecraft will have completed 88 orbits. These orbits shall have a uniform distribution and will be separated by 242 km at the equator. We have simulated and analyzed these data with the intent of determining the expected improvement in the gravity field. The results of this work are summarized in Fig. 3 for a limited 6 × 6 gravity field model. This is done by comparing the GC results with the current best estimate of Mars' gravity field.[5] This figure indicates that significant improvement in the Mars global gravity field can be expected as a result of this data set. During flight operations, we have allocated 30 working days for the development of a new gravity field model. This short-term analysis is required because we want the mapping operations to benefit from the improved gravity field accuracy as soon as possible. Results of this analysis as well as more details on procedure can be found in Ref. 6.

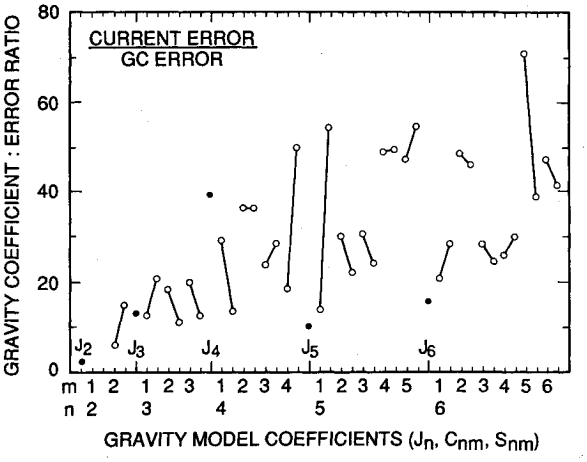

Fig. 3 Improvement in a truncated sixth degree (n) and order (m) gravity field due to the GC strategy.

Orbit Determination During the Mapping Phase

Throughout the mapping phase, spacecraft location errors for both reconstruction and prediction have been evaluated. For reconstruction errors, simulated Doppler over a typical tracking pass of 10-h duration have been analyzed. Because of the shortness of the data arc, only a limited number of parameters can be updated or estimated. Typically, this includes the six initial conditions (position and velocity at the analysis epoch) and several gravity field parameters. Conservatively, we have assumed Doppler data (for a 60-s average) noise of 1 mm/s. Estimated parameter errors are calculated as follows:

$$\Lambda = (A^T W A + \bar{\Lambda}^{-1})^{-1} \quad (1)$$

where A contains numerically evaluated partial derivatives of the tracking data with respect to the estimated parameters, W is a weighting matrix (usually diagonal) specifying the data quality, and $\bar{\Lambda}$ represents the a priori error for each of the esti-

mated parameters. The Λ is usually called the estimated parameter covariance matrix.

Experience has shown that the results of Eq. (1) are generally optimistic, and thus those errors are regarded as formal errors. In this OD study, we must deal with realistic errors because of the many design decisions made throughout the Mars Observer project based on these results. Accordingly, the estimated covariance has been supplemented by a term that allows for the influence of error by effects that do not directly enter the estimation process. This could be due, for example, to Earth-Mars ephemeris errors. Mars' ephemerides may not be able to be improved by the Doppler data acquired during mapping. Yet it is important to consider how Mars' position and velocity errors affect our knowledge of reconstructing the spacecraft's orbit. This process is called consider analysis and results in a consider covariance matrix:

$$\Lambda_c = \Lambda + S\,\tilde{\Lambda}_c\,S^T \qquad (2)$$

where S is the sensitivity matrix (numerically evaluated partial derivatives of estimated parameters with respect to consider parameters). These equations form the basis of the error assessments in this article.

Reconstruction errors differ from prediction errors insofar as the former are determined directly from radio tracking data whereas the latter are propagated in time beyond the data arc. In this case, the data are generally acquired over a 10-h interval, whereas for propagation the spacecraft location errors are evaluated at 14–21 days past the analysis epoch. Generally, for reconstruction, gravity field errors dominate, whereas for prediction, atmospheric density errors dominate (primarily through downtrack errors).

Estimates of Mars' atmospheric density throughout the mapping phase are given in Fig. 4. These are given at a mean or 50% confidence level as well as several other confidence levels. For example, on Dec. 6, 1993, the 50 and 90% confidence levels for the atmospheric density at the Mars Observer orbit are 0.17×10^{-13} kg/m^3 and 0.57×10^{-13} kg/m^3, respectively. The source of the model, inputs, and assumptions used to produce this figure are given in Ref. 7.

Throughout mapping, the nominal plan is to acquire one tracking pass of Doppler per day with an additional pass every third day for high-rate telemetry data acquisition. During special circumstances, such as when the spacecraft's orbit is seen edge on from Earth, station coverage shall increase. We shall

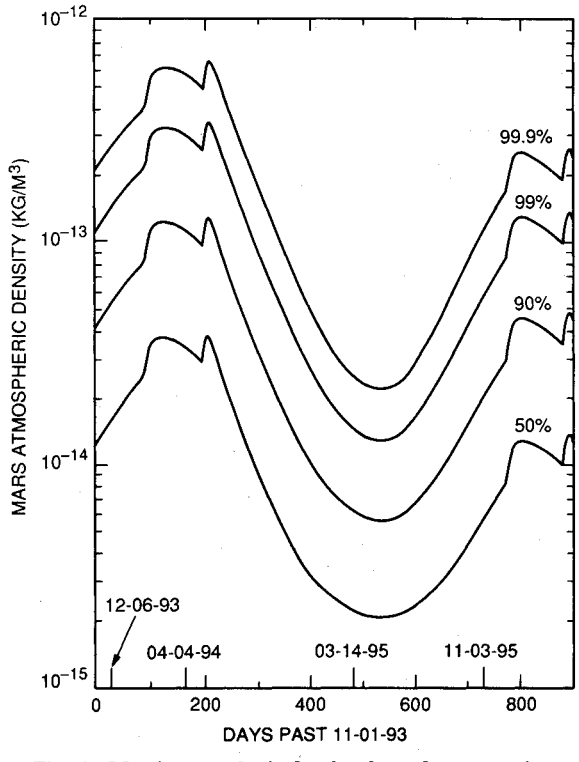

Fig. 4 Mars' atmospheric density throughout mapping.

Table 9 Inputs and assumptions for analysis of two cases (Dec. 6, 1993, and April 4, 1994) studied during the mapping phase

Quantity	Case 1, Dec. 6, 1993	Case 2, April 4, 1994
Doppler data	One tracking pass ($N=95$)	One tracking pass ($N=94$)
Doppler count-time, s	180	180
Doppler noise, mm/s, for a 1-min count-time	1	1
Estimated parameters	Position and velocity Local gravity field modeled as gravity anomalies	Position and velocity Atmospheric density
Consider parameters	Sixth degree and order global field Local gravity field due to gravity anomalies Atmospheric density Solar radiation pressure Angular momentum desaturation Tracking station coordinates *GM* (Mars) Mars-Earth ephemeris	Sixth degree and order global field Local gravity field due to gravity anomalies — Solar radiation pressure Angular momentum desaturation Tracking station coordinates *GM* (Mars) Mars-Earth ephemeris
Comments	This case is near the beginning of mapping and just before solar conjunction. Current global gravity field model errors have been utilized.	This case occurs at the maximum of the atmospheric density (see Fig. 4). We utilized the expected gravity field model errors resulting from the GC analysis (for both the global and local gravity field).

Table 10 Reconstructed and predicted spacecraft position errors, km, 1 σ for two cases during the mapping phase

Epoch, T_0; days past T_0	Radial	Cross-track	Down-track	Comment[a]
Dec. 6, 1993	0.018	1.34	1.30	Utilize current gravity
7	0.32	1.26	7.34	model and 90% atmos-
14	1.31	1.43	24.8	pheric density.
21	2.48	1.48	53.6	
April 4, 1994	0.005	0.24	0.05	Utilize GC gravity model
7	0.038	0.26	7.08	and estimate the atmos-
14	0.13	0.29	29.4	pheric density directly
21	0.22	0.26	66.8	from the tracking data.

[a]The 90% density error corresponds to a 1.28-σ high density and influences primarily the downtrack error. Propulsive maneuver execution errors have not been accounted for. Note that Ref. 8 provides more detail on the atmospheric drag perturbation acting on Mars Observer. However, it applies to a previous definition of the mapping orbit. The current orbit is approximately 17 km higher.

summarize the OD results for two cases during the mapping phase. The first is denoted by the epoch Dec. 6, 1993, which occurs near the beginning of mapping and just before solar conjunction. Since the results of the GC are not yet available, we use current gravity field model errors. Also a priori atmospheric density errors are taken from Fig. 4. These densities cannot be improved by analysis of the drag perturbation acting on the spacecraft because the gravity field model is too uncertain. Table 9 provides a summary of inputs and assumptions used in the analysis.

The OD results for two cases, due to the analysis of Doppler under the above conditions, are given in Table 10. For the Dec. 6, 1993, epoch, the largest position errors for reconstruction are in the crosstrack and downtrack directions. Crosstrack errors are in a direction normal to the instantaneous orbital plane of the spacecraft (that is, in the $r \times v$ direction). Downtrack errors are in the instantaneous orbital plane and in the direction of motion (that is, in the $r \times v \times r$ direction). Prediction errors are given for 7, 14, and 21 days past the analysis epoch. As shown, the errors in the downtrack component of position (DT) rise dramatically and are due almost exclusively to the atmospheric drag. Errors in the crosstrack component of position (CT) are fairly constant. The radial errors also show an appreciable increase but remain relatively small.

Position errors are also given for a second case identified by the analysis epoch, April 4, 1994. The reconstructed errors are much smaller than those of the previous case because we have used smaller gravity field errors. This is due to the GC results mentioned previously. DT errors show a similar growth pattern when compared with the Dec. 6, 1993, case. This is because a priori density errors are larger for April 4, 1994 (see Fig. 4). Furthermore, even though we solved for a mean atmospheric density, only a small improvement was realized. Radial errors remain relatively small over the entire 21-day prediction interval.

Conclusions

Based on the orbit determination analyses summarized in this article, a navigation plan has been developed to 1) assess OD accuracies throughout interplanetary cruise with emphasis placed on supporting the four TCMs, 2) determine targeting accuracies at encounter in preparation for the MOI maneuver, 3) evaluate OD errors throughout the orbit insertion phase during which the spacecraft shall be maneuvered from a highly elliptical to a nearly circular, short-periodic orbit, 4) prepare a GC plan and establish the expected improvement in the gravity field model, and 5) determine OD accuracies throughout the mapping phase. The mapping phase information is required for reconstruction of the spacecraft's orbital motion used primarily for scientific data analysis. In addition, prediction information over 14–21 days is required for navigation, science, and sequence planning purposes. All of these results with the supporting background is given in much greater detail than is permitted in this overview in Ref. 9.

Acknowledgment

The research described in this paper was carried out by the Jet Propulsion Laboratory, California Institute of Technology, under a contract with the NASA.

References

[1]Melbourne, W. G., and Curkendall, D. W., "Radio Metric Direction Finding: A New Approach to Deep Space Navigation," AAS/AIAA Paper 77-170, Sept. 1977.

[2]Border, J. S., Donivan, F. F., Finley, S. G., Hildebrand, C. E., Moultrie, B., and Skjerve, L. J., "Determining Spacecraft Angular Position with Delta VLBI: The Voyager Demonstration," AIAA/AAS Paper 82-1471, Aug. 1982.

[3]Ries, J. C., Eanes, R. J., Huang, C., Schutz, B. E., Shum, C. K., Tapley, B. D., Watkins, M. W., and Yuan, D. N., "Determination of the Gravitational Coefficient of the Earth from Near-Earth Satellites," *Geophysical Research Letters,* Vol. 16, No. 4, 1989, pp. 271–274.

[4]Smith, D. E., and Fricke, S., "A New Determination of Mars GM," *EOS Transactions,* American Geophysical Union, Vol. 72, No. 17, 1991, p. 181.

[5]Balmino, G., Moynot, G., and Vales, N., "Gravity Field Model of Mars in Spherical Harmonics up to Degree and Order Eighteen," *Journal of Geophysical Research,"* Vol. 87, No. B12, 1982, pp. 9735–9746.

[6]Esposito, P., Demcak, S., and Roth, D., "Gravity Field Determination for Mars Observer," AIAA/AAS Paper 90-2945, Aug. 1990.

[7]Culp, R. D., and Stewart, A. I., "Time-Dependent Model of the Martian Atmosphere for Use in Orbit Lifetime and Sustenance Studies," *Journal of the Astronautical Sciences,* Vol. 32, No. 3, July–Sept. 1984, pp. 329–341.

[8]Esposito, P. B., and Demcak, S., "Atmospheric Drag Perturbations on the Mars Observer Orbiter," American Astronautical Society, AAS Paper 89-405, Aug. 1989.

[9]Esposito, P. B, "Mars Observer Project Navigation Plan," Jet Propulsion Laboratory, Pasadena, CA, JPL D-3820 (JPL Internal Document), June 1990.